Quest Journals
Journal of Research in Environmental and Earth Sciences
Volume 7 ~ Issue 11 (2021) pp: 56-68
ISSN(Online) :2348-2532
www.questjournals.org

Research Paper

Investigation of Soil Liquefaction Susceptibility Using Seismic Refraction Method; a Case Study of Opolo Town, Bayelsa State, South-Southern Nigeria.

George, Godwin C[1]. and Ogobiri, Godwin[1]
[1](*Department of Physics, Niger Delta University, Wilberforce island, Bayelsa State, Nigeria)*

ABSTRACT
Due to the Earth tremors that occurred on July, 2016 at Bayelsa state, south southern Nigeria, it is now necessary to study the true seismicity of the areas such as OPOLO that is around the likely epicenter of such event. Liquefaction susceptibility of the soils at 8 m and 15 m depth was investigated using the simplified procedure. Seismic refraction method was predominantly used to determine the shear-wave velocity, the shear-wave velocity was also corrected and used to determine the cyclic resistance ratio which are; 0.06 and 0.16 for 8 and 15 m respectively. The cyclic stress ratio was computed as 0.23 and 0.21 for 8 and 15 m respectively. The safety factor was computed in terms of Mw = 5.5 and 7.5. For Mw = 5.5; it is 0.80 and 2.39 for 8 and 15 m respectively while Mw = 7.5, it is 0.27 and 0.80 for 8 and 15 m respectively. From the result achieved, soils at 8 m depth is susceptible to liquefaction with respect to Earthquake (Mw = 5.5) while with respect to earthquake (Mw = 7.5), soils at both depth (8 and 15 m) will liquefy.
KEYWORDS; liquefaction, factor of safety, geophysics.

Received 17 November, 2021; Revised: 29 November, 2021; Accepted 01 December, 2021 © The author(s) 2021. Published with open access at www.questjournals.org

I. INTRODUCTION

Earthquakes produce seismic waves that travel through the ground. An earth tremor is a little or short-lived movement or shake in the Earth's surface. Vacuum suction in the soil is able to increase the pressure on the particles when the water around them is reduced, thereby keeping the soil stable. When water pressure is present at many levels, soil particles jostle against one another, diminishing the soil's ability to support weight and increasing the chance of soil collapse. The earth therefore behaves like a viscous liquid for a short time. This is known as soil liquefaction. Ground liquefaction is a significant hazard, since it may cause damage to both people and the structures they inhabit. In all, this damage includes the displacement of houses and buildings, the formation of buckled roads and driveways, the destruction of bridges, the lifting of septic tanks and drainage pipes, and the lifting of other floating constructions (Beroya & Aydin, 2007). Liquefaction is often observed in loosely soaked sand, although it may also be seen in gravel and silt without plastic (Sahar & Fereydoun, 2015). As seismicity is more common in saturated loose soil formations, it is critical to explore the liquefaction potential of soil at larger depths.Numerous studies on the potential or probability of soil liquefaction have been performed during the past two decades. Idriss and Seed (1971) developed a technique for assessing liquid resistance in Alaska and Nigatta in 1964 after the earthquakes. It was based on SPT-N data. Tokida, Iwasaki, Tatsuoka, Watnabe, Yasuda, and Sato (1982) outlined several ground liquefaction research methods using Japanese earthquakes. In the 1988 study by Liao and Whitman, more data was used to evaluate the soil liquefaction potential in Japan. For their examination of liquefaction-related building damage after the 1999 earthquake, Mollamahmutoğlu, Kayabali, Bayaz, and Kolay (2003) used a soil liquefaction test method. Yilmaz and Yavuzer (2005) conducted a survey in Yalova City after a devastating earthquake to produce a liquefaction and susceptibility map of Turkey. According to Anbazhagan (2009), an evaluation of soil liquefaction potential was conducted using a simple technique, while the risk of Bangalore soils in South India was mapped. Ozcep, Karabulut, Ozel, Imre, Ozcep and Zarif (2014), Firat, Arman and Kutanis (2009), Shahri, Esfandiyari, and Rajablou (2012) have produced liquefaction studies that are similar to the current research.

These vibrations and cracks were seen in Yenagoa and the nearby areas of Bayelsa and are believed to have caused the structural failures shown in Fig. 1.1. The following, however (A, B, C, and D), this kind of tremor has Mw values ranging from 2.6 to 3.0, as Nwankwoala and Orji detail (2018). Earthquakes in and near

Yenagoa have increased in frequently in recent years. Previously, it was believed that the state of Bayelsa was far less seismically active than it really is. Seismic activity has been rising dramatically, and this is a clear indicator of how big the next earthquakes will be. The region around Yenagoa has witnessed an astonishing growth in population in the past two decades. The danger of earthquakes in which a big population is involved has been raised to an area of high geological risk. But, while the threat is immediate. the knowledge of the earthquake hazard in the public is usually very low. In addition, the state or nation is not equipped to deal with a big earthquake. There are no mechanisms that are national of early warning nor there suitable building regulations that may result in the development of resistant buildings.

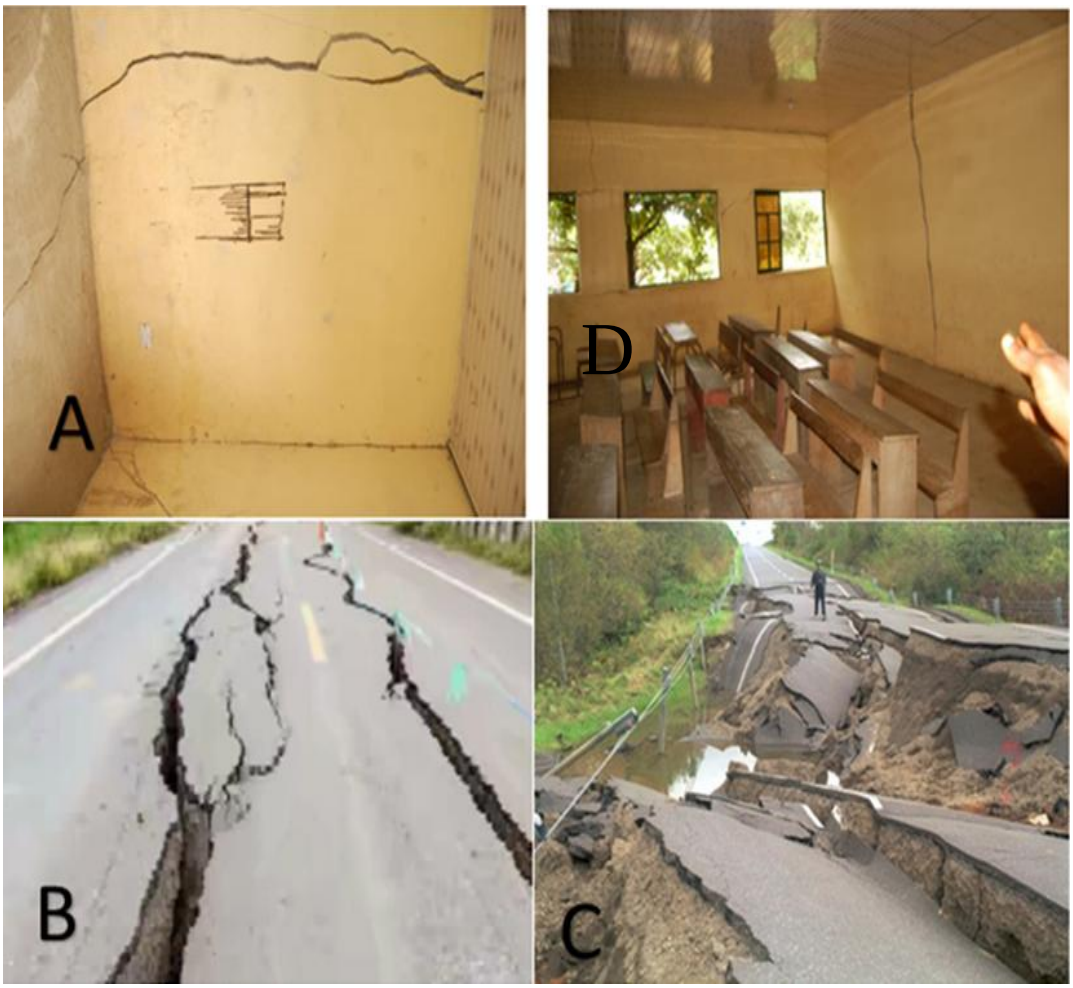

Fig 1.1: (A & D) Wall cracks in Tombia primary school building (B) Road crack caused by earth tremor in Igbogene major road. (C) Road crack caused by earth tremor in Ikarama, Okordia clan, Bayelsa state.

Notwithstanding the dangers presented by earthquakes in soil liquefaction there has been inadequate attention to the determination of soil liquefaction and has therefore been largely insufficient in the Niger Delta. Currently, the liquefaction potential index in and around Yenagoa is still unconscious.
In this research, liquefaction potential index data from technical seismic refraction and electro-resistant method were investigated in Yenagoa and the surroundings.

II. GEOLOGY OF THE AREA

Yenagoa is the site in Nigeria's southern sedimentary basin. It's the capital of Bayelsa state. The location of the research spans an area of about 50 km^2 and is a metropolis in Yenagoa. The lengths of the Yenagoa 00 6° 25 10.53 ″ and 006 ° 1003.07 East of the Meridian and latitudes 05 ° 2′ 25. 53″ and 04 ° 51′39.73 North of equator (Okiongbo, Oboshenure and Amakiri , 2019).

Geographically, the region of the Yenagoa is situated in the coast area of the newly formed Niger Delta Basin (see Fig. 1.2) where the surface area of the soil slopes quite smoothly in the sea (Akpokoje and Etu-Efetor, 1987). A tropical rainforest environment with dry season and rainy season is the research region. Between November and March the dry season starts, while April through October the wet year. The average annual precipitation is about 4,500 mm and roughly 85% of wet seas falling in average annual precipitation.

The temperature ranges from 25 to 32 °C. The primary profession of the people is agriculture and fisheries (Akpokoje, 1986; Okiongbo et al., 2019).

The region of research is situated in freshwater marshes, alluvial ponds, swamps, sinuous belt and geomorphic units of the Niger Delta. The Niger Delta mostly comprises of the Holocene and top deposits of the contemporary delta. The Holocene alluvial deposits include particle size profiles consist of a succession of finely sanded and clay sand that indicates a river deposition environment (Amajor, 1991). The finely seeded silts and clay that border the sandy series of bases are frequently called aquitards on the surface (Uko, Ekine, Ebeniro, Charlse and Ofoegbu, 1992). The aquitard thickness at the surface ranges between <5 and roughly 12 meters, and the permeability is highly heterogeneous owing to its variable contents of clay, silt and fine sand. If it is impermeable and thick, the aquitard at the surface forms a containment unit that inhibits percolation of precipitation into the alluvial water table. Groundwater in the area runs north to south (Akpokodje, 1986).

Three main lithostratigraphic subterranean units are found in the Niger Delta (Short & Stauble, 1967), these are the Benin, Agbada, and Akata groups, respectively from top to bottom. The Benin formation is the principal aquifer of river origin. Groundwater in the Benin formation is found mostly under unrestricted circumstances. Abam (1999) stated that Benin's sediment deposit is about 2,100 m thick in the course of the tertiary and quaternary late start. The sediments are unconsolidated, lenticular and include coarse to medium-sized seed sands with isolated clay and shale intercalations. Gravel and caulk are components that are little. The sands are poorly organized and cemented (Mbonu, Ebeniro, Ofoegbu and Ekine, 1991). The presence on the side of thin, clay beds produces discontinuities which lead to locally perched aquifers (Amajor, 1991). The aquifer is immediately charged in the research region by rainfall infiltration. In the Niger delta, the water table is really close to the surface in many regions but also susceptible to seasonal fluctuation; in the dry season it is around 3 - 4 m high while in the rainy season it is upward. Groundwater is the major water supply for 80% of the research area's population (Okiongbo, et al., 2019).

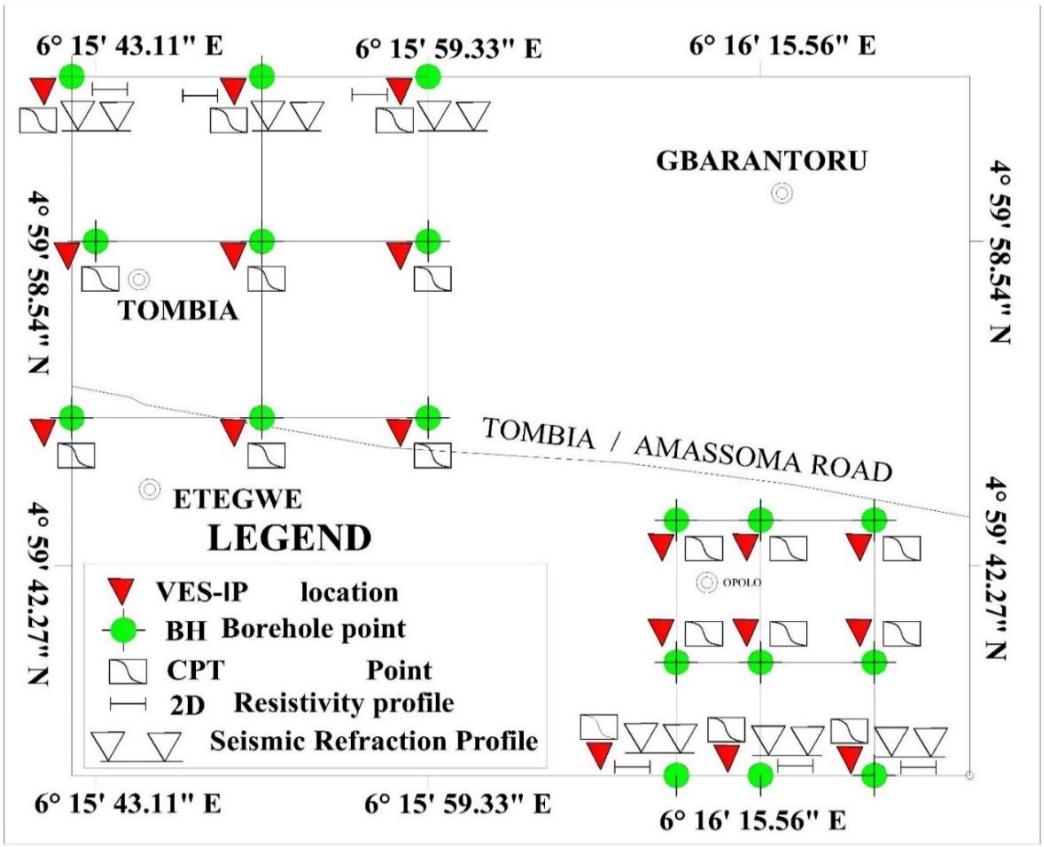

Fig. 2: Map of study area showing seismic refraction survey.

3.1. Instrumentation

- 12-channel seismometer; (ABEM TERRALOC MK 6)
- 13 Vertical geophones of 10 Hz.
- Easy Refract, 2D/3D seismic interpretation, modelling, inversionand seismic processing program.
- 25 kg Hammer with an energy seismic base plate.

• Geophone cable.
• Trigger geophone cables
• A battery of 12 volts
• The field survey tapes are two, each 100 meters long.
The refractive seismic field survey was set up with a cross-clearance machete and field log.

3.2 Data acquisition

Each location has three seismic refraction lines(Fig. 4). When collecting data, we usually attempt to carefully monitor the horizontal or near horizontal surfaces of the soil in order to approach the horizontal bed hypothesis by selecting our survey parameters. The survey was conducted in a straight line with the source and receivers. Geophones were placed at 5 meter intervals at different locations of extraction and linked with a seismic signal cable, as illustrated in figure 4.

Fig. 3: Seismic refraction survey equipment. (a) Digital seismograph ABEM Terraloc MK6, (b) Seismic land cables, (c) sledgehammer (d) vertical geophone, (e) reel wire, and (f) GPS Device, (Rami, 2014)

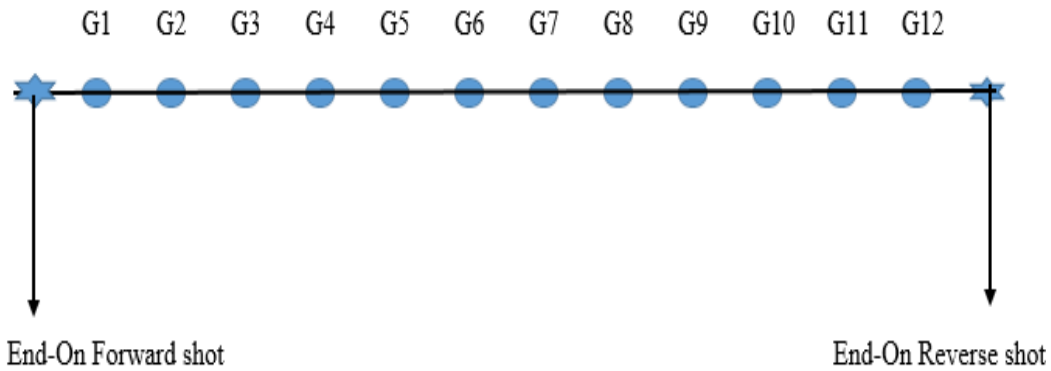

Fig 4: Seismic Field Survey Geophone Layout.

Digital seismograph ABEM Terraloc MK6 has been used for the collection, has a broad range of sampling rate and the window time length is 204.8 ms, where the sample rate used is 100 µs (Rami, 2014).

After the device has been set up, the operator will set up the digital seismograph and validate the expectation of the shooter. The operator monitored the noise conditions of the seismograph and fired the rounds with the minimum or acceptable noise possible. Each shot is produced byhitting a 25kg hammer on a rubber plate. The recording device was armed and the first shot was fired 30 meters from the first geophone (End-on forward shot). It was fired multiple times at 5 meters interval until it reached 115m or 30m after the last geophone (situated at 85m). The seismic signal (seismogram) was extracted from the seismograph and transported for further processing, modelling, inversion and interpretation to the workstation.

3.3 Data processing:

3.3.1 Frequency filtering:

Filtering aims to eliminate undesirable fluctuating noise frequencies. Unwanted noise sources may include road transport, wind-induced noise and footsteps in this research and can usually be filtered without losing any seismic signals (Asokhia, 1984).

First step of filtering was done on the raw data by the application of a low cut-off (High pass) of 75 Hz and a high cut-off (Low pass) of 200Hz. The refraction event was improved by using a 15 dB gain filter.

3.3.2 Picking the First Arrivals and Creating the Travel Time Curves:

The first arrivals were picked manually once the raw data were filtered. The timing of arrival of the first event is the important information from the seismograms obtained. If the signal-to-noise ratio is poor, it may be difficult to pick the first arrivals. The first arrivals should thus be followed, chosen and connected again from the peak seen on the trace of the last geophone to the trace of the first geophone, this is better done after appropriate amplification has been carried out on the traces. The first arrivals were selected using geophysical software(Easy Refract). (Figure 5).

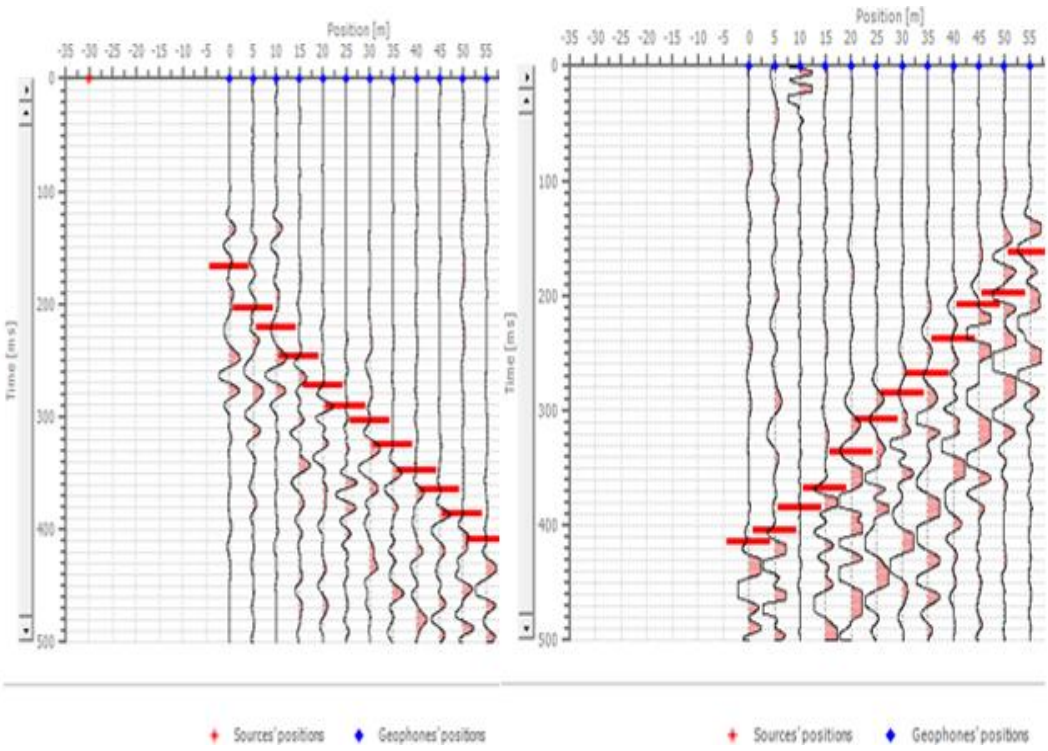

Fig.5: Forward and Reverse picking of Arrivals in Opolo1 Data.

The times of the first arrivals obtained from the manual pickingwas now plotted against the distances of the geophones from the source position. Thus, the diagram is called the travel time curve or the time-distance curve, and the velocity of the line or layer has been determined as the inverse of the slope. In essence, steep slopes correspond to slow velocity, while gentle slopes correspond to high velocity. Basically the first and last shots were used to produce the travel time curves. (Fig. 6). The travel time curve was further processed to obtain the processed travel time curve, it is with this curve that the layer thicknesses were determined using the Easy Refract geophysical software which is based on the GRM method.

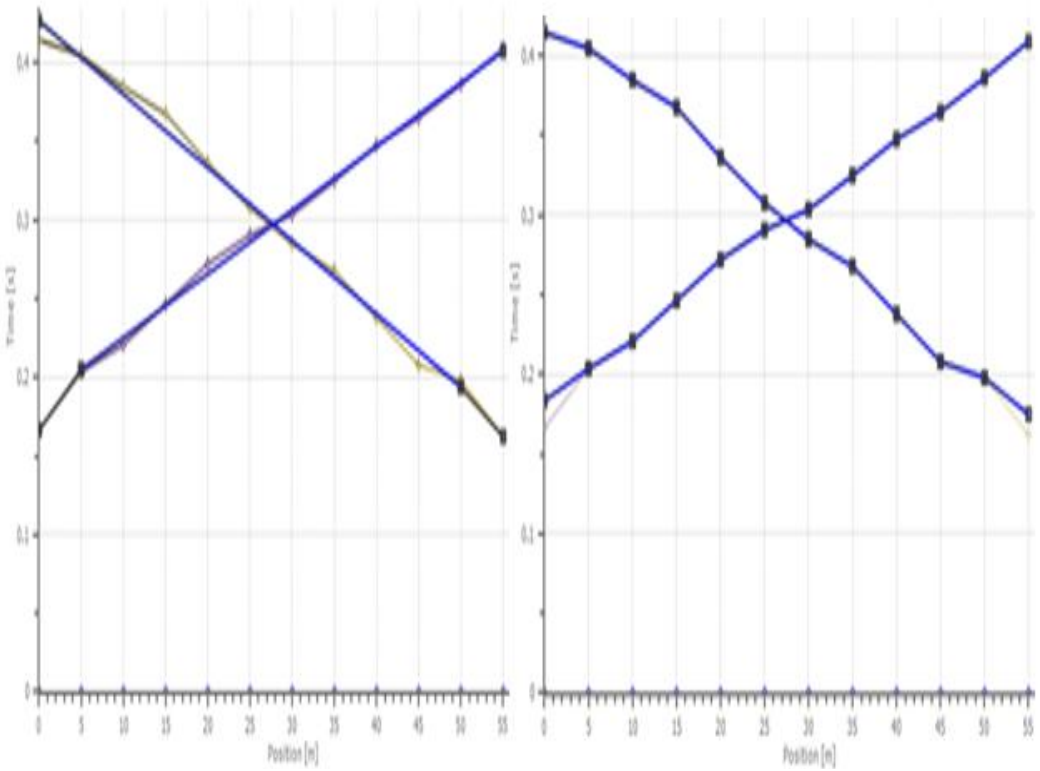

Fig. 6: travel-time curve and processed Travel-time curve of Opolo-1 data

3.4. Cyclic stress ratio (CSR) Assessment

The cyclic stress ratio is the cyclic load level produced by the earthquake, it is calculated using the (Seed and Idriss, 1971) relation. The cycle stress ratio is estimated on the basis of the knowledge of certain parameters, particularly the pore water pressure, total overburden pressure, effective overburden pressure.

a) Porewater pressure; This is the pressure of soil or rock groundwater.

$$p = \gamma\left(z - z_{o}\right) \tag{1}$$

Where z is the depth in meters, z_o is the depth of the water table and is the unit weight of water (9.8 KN/m^3).

b) Total overload stress: This is the pressure or stress exerted on a formation at a given depth due to the total weight of rocks and fluids above the depth.

σ_v = Total vertical overload constraint, it will be calculated using the relation;

$$\sigma_{v} = \sum \gamma_{t} z \tag{2}$$

Where, γ_t is the total weight of the soil unit and z is the depth in meters (Song and Mikell, 2013).

c) Effective overload stress: this is the stress that occurs when the soil is subjected to a certain load and transfers the load to the water in the pores and grains of the soil.

$$\sigma^{1}_{v_{v}} = \sigma_{v} - p \tag{3}$$

Where p is the pore water pressure calculated by the equation;

The cyclic stress ratio is calculated using the formular of Seed and Idriss (1971);

$$CSR = 0.65\left(\frac{a_{\max}}{g}\right)\left(\frac{\sigma_{v}}{\sigma^{1}_{v}}\right) r_{d} \tag{4}$$

where

A_{max} = the peak horizontal ground surface acceleration due to an earthquake

g = acceleration due to gravity,

σ_v = Total vertical overburden stress, $\sigma^1_{v_v}$ = Effective overburden stress

R_d = stress reduction factor, it can be estimated from the, (Liao and Whitman, 1986) relations

$$r_d = 1.0 - 0.00765 \times z \quad \text{for } z \leq 9.15\text{m} \quad (5)$$

$$r_d = 1.174 - 0.0267\ z \quad \text{for } 9.15 < z \leq 23\text{m} \quad (6)$$

$$r_d = 0.744 - 0.008\ z \quad \text{for } 23 < z \leq 30\text{m} \quad (7)$$

$$r_d = 0.5 \quad \text{for } z > 30\text{m} \quad (8)$$

3.5. Assessment of Cyclic Resistance Ratio (CRR) using stress-corrected shear wave velocity.
This is estimated using the relation (Andrus and Stokoe, 1997);

$$CRR = 0.022\left(\frac{v_{sl}}{100}\right)^2 + 2.8\left(\frac{1}{\dot{v}_{sl} - v_{sl}} - \frac{1}{\dot{v}_{sl}}\right)MSF \quad (9)$$

Where V_{sl} is the overburden-stress corrected shear wave velocity$\dot{V_{sl}}$ and is the limited upper value of V_{sl} for the occurrence of liquefaction, MSF is the magnitude scale factor which is 1 and 2.20 for earthquakes of magnitude 7.5 and 5.5 respectively (Andrus, Stokoe , Chung and Juang , 2003). The stress-overload corrected shear wave is calculated using the equation;

$$V_{SL} = V_S\left(\frac{P_a}{\sigma_v{}^1}\right)^{0.25} \quad (10)$$

Where P_a is atmospheric pressure, i.e. 100 KP_a, Vs is the shear wave velocity obtained from the processed refraction seismic data and σ_V^1 is the effective overload stress in KPa.

3.6. Determination of the Safety Factor
The Liquefaction Safety Factor (FOS) is primarily used to quantify the liquefaction potential. FOS is defined as the ratio between CRR and CSR. If this ratio is equal to or greater than one (1) for a given site, then the site is against soil liquefaction, but if FOS is less than one (1), the site is subject to soil liquefaction. .

$$FOS = \frac{CRR_{7.5}}{CSR} \quad (11)$$

Where CSR is the Cyclic Stress Ratio and CRR is the Cyclic Resistance Ratio (Liquefaction resistance).

III. RESULT AND DISCUSSION

The quantitative result of the Seismic refraction data obtained from the three (3) points in the location of the study area are presented as model result in Table 1. The Time-intercept method and the General reciprocal method (GRM) were used and the results are presented below. In Table 1, the P-wave velocities, S-wave velocities and depth of the various layers obtained in the study area are also shown.

4.1. Result using Time-intercept method.

Result of the intercept-time method is shown in Fig. 7 – 9. These Figures shows that two-layer plots were obtained in all the three (3) points in each of the locations. Also displayed in the Figures are the integrate p-wave velocity of the forward and reverse shot at the six points. Average thickness and P-wave velocity of both shots (forward and reverse) were computed and presented in Table 4.2. These model results were used for the computation and determination of the liquefaction parameters.

At the location of Opolo, the thickness of the first layer varies from 8.3 to 11.1 m, with the velocity of P-wave in range of 185 to 201 m/s, the second layer has a velocity of P wave (Vp) in the range 244 to 386 m/s, the velocity of the S wave (Vs) , was obtained by dividing the velocity of the P wave by 1.7 (Akinshipe , Kenneth and Geoffrey, 2021) , it varies between 109 - 118 m /s in the first layer and 143 - 227 m/s in the second layer.

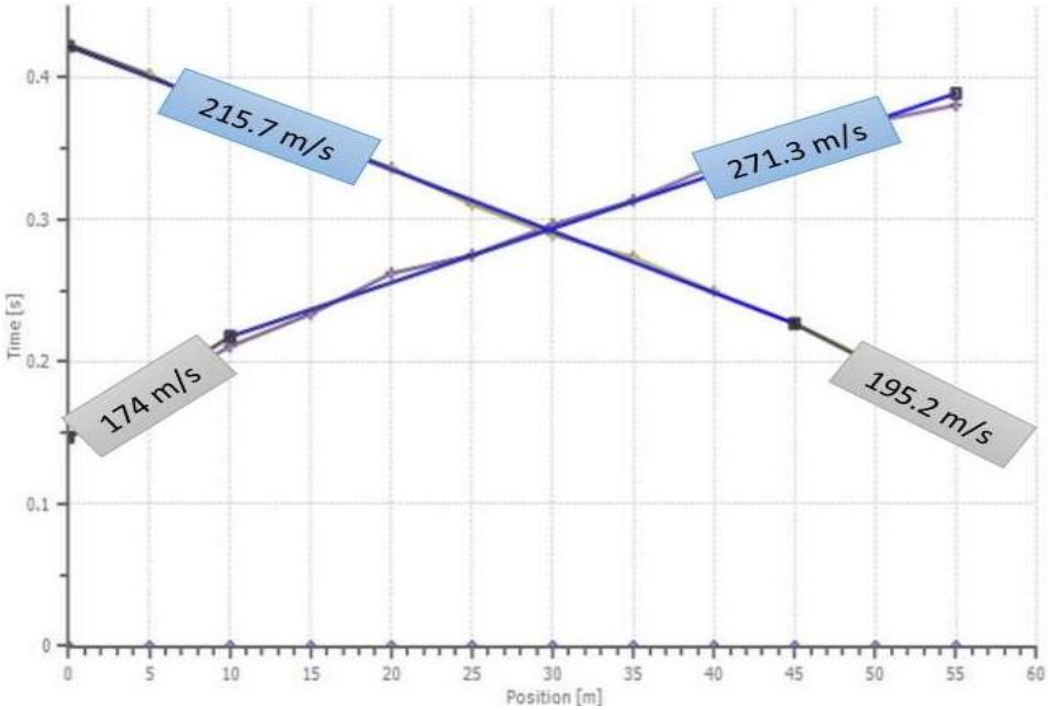

Fig 7:Time-intercept interpretation of Opolo-1 seismic refraction data.

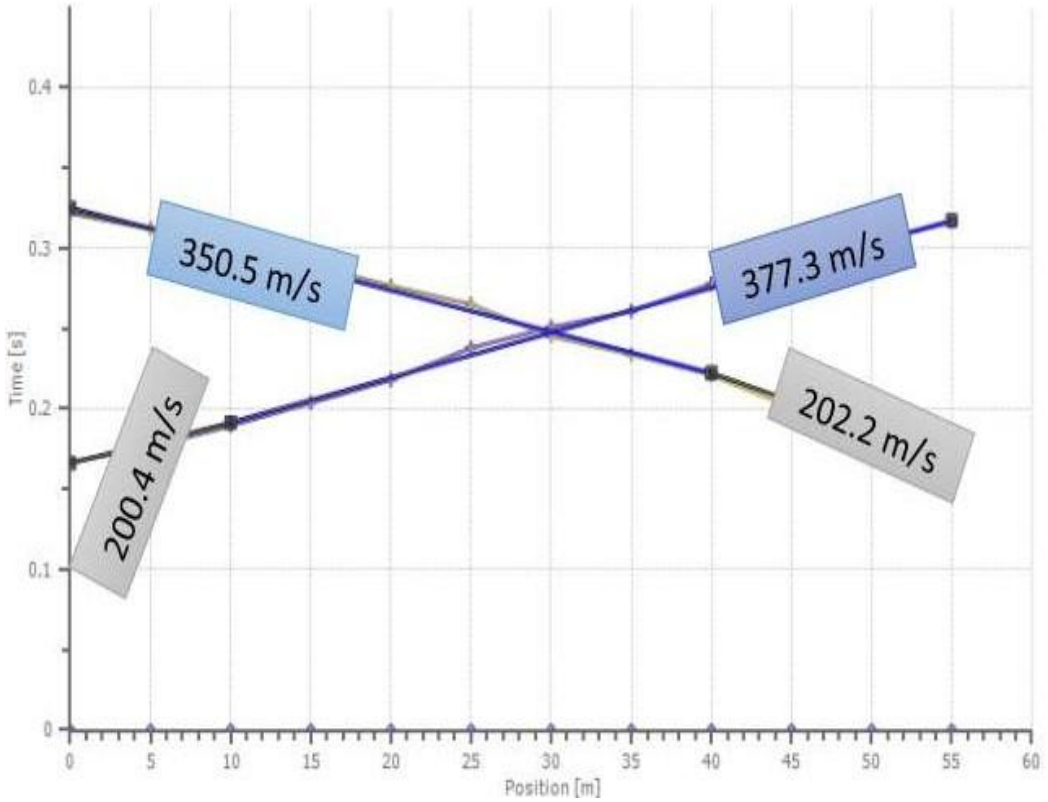

Fig 8: Time-intercept interpretation of Opolo-2 seismic refraction data.

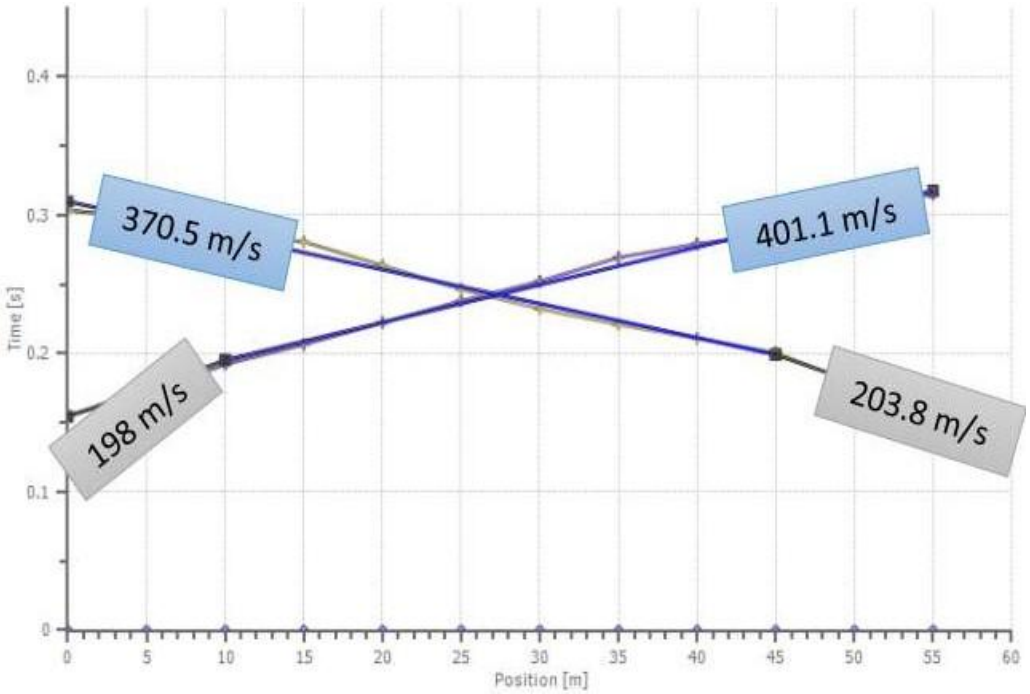

Fig 9: Time-intercept interpretation of Opolo-3 seismic refraction data.

Table 1: quantitative interpretation of seismic refraction data

Location	Layer depth (m)		Layer body-wave velocity (m/s)			
	1	2	Vp (m/s)	Vp (m/s)	Vs (m/s)	Vs (m/s)
			1	2	1	2
Opolo-1	8.3	----	187	244	109	143
Opolo-2	11.1	----	201	369	118	217
Opolo-3	11.0	----	201	386	118	227

4.2 Velocity Modelling

The velocity modelling is a product of the General Reciprocal Method applied in this study. It shows the distribution of the compressional wave velocity along the line of survey. It is been processed from the initial velocity model gotten from the time-intercept method (processed travel-time curves). The velocity model is the best in terms of displaying gradational vertical changes in velocity and also lateral changes in velocity, in order words, a 2D velocity model is realized. The velocity modelling inversion was done using Easy Refract software. The horizontal axis represent distance in meters while the vertical axis represent elevations in meters. Fig. 10 - 12 display the 2D velocity model of Opolo location.

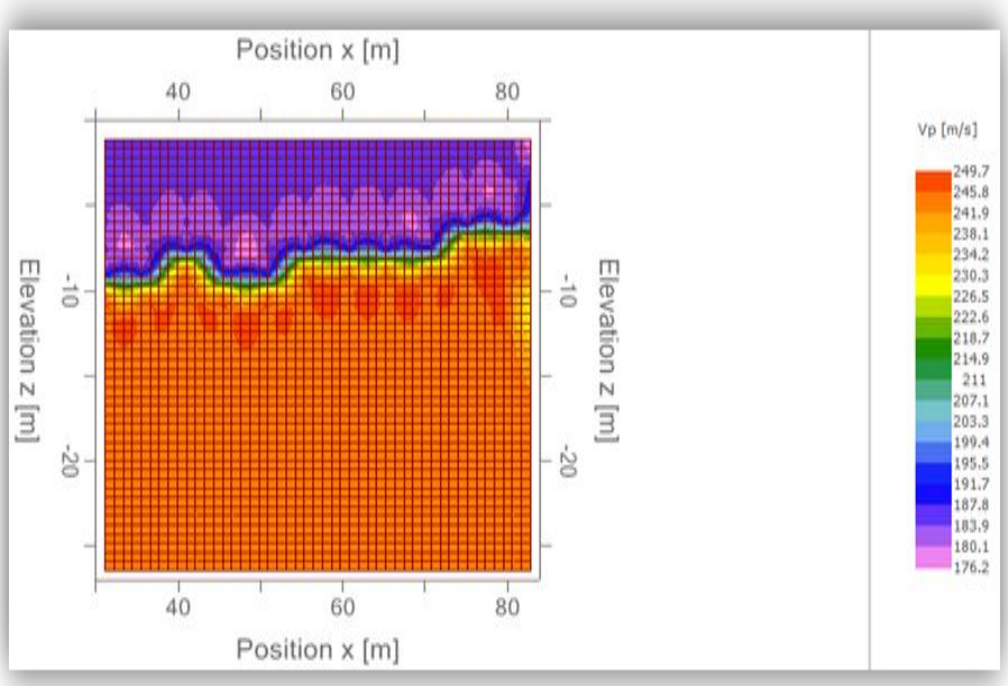

Fig.10: 2D velocity model of opolo-1 data

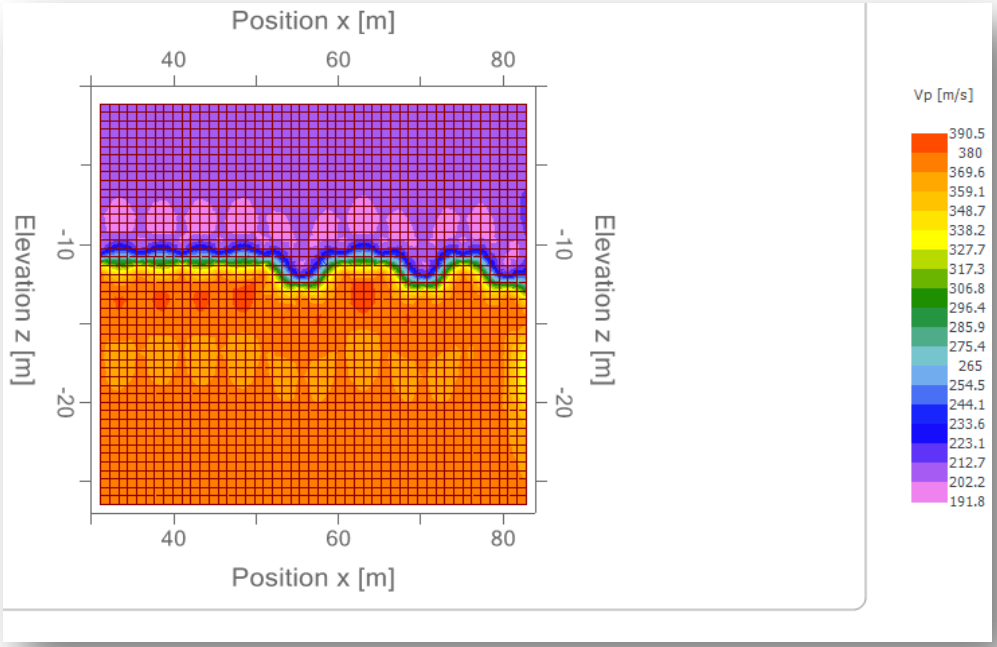

Fig. 11: 2D velocity model of Opolo-2 data

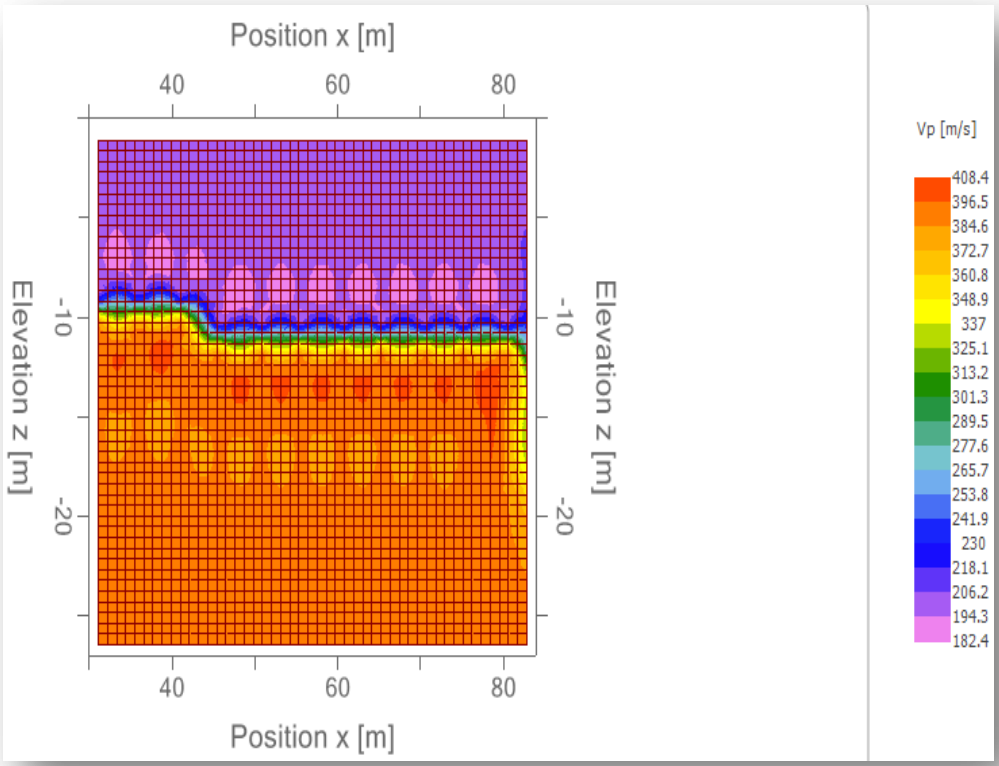

Fig. 12: 2D velocity model of Opolo-3 data

4.3. Liquefaction parameter using corrected shear-wave velocity

Avearge velocity of shear-wave(Vs) was estimated from seismic refraction shear wave velocity data presented in Table 1in study site. These average shear-wave velocities were further subjected to correction using Equ. 10, through which the cyclic Resistance ratio (CRR) was determined using Equ. 9. Factor of safety (FS) with respect to Mw= 5.5 and 7.5 of Opolo at both depth (8 m and 15 m) were also computed and determined. Results of all the above are presented in Table 2.

In Opolo location, the average corrected Shear-wave velocities of both depth (8 m and 15 m) are 127.29 m/s and 185.22 m/s respectively. Using the above values, the computed CRR values at 8 and 15 m depths are 0.063 and 0.164 respectively.

Factor of safety (FS) displayed in Table. 4.7 can be explained as follows: when the magnitude of the tremor is 5.5 (Mw = 5.5), while in Opolo location, only the soil at 8 m depth is prone to liquefaction (0.804), the soil at 15 m depth is not prone to liquefaction because its safety factor is greater than one (2.391). When the Magnitude of the tremor is 7.5 (Mw = 7.5), the soils at both depth (8 m and 15 m) will be prone to liquefaction because their factor of safety are all less than one (Table 4.7).

Table 2: liquefaction parameters using seismic refraction method

Depth (m)	Average shear-wave velocity (Vs)	Average corrected shear-wave velocity (m/s)	Cyclic resistance ratio (CRR)	Cyclic stress ratio	Factor of safety (FS), Mw = 5.5	Factor of safety (FS), Mw = 7.5
8	115	127	0.06	0.23	0.80	0.27
15	196	185	0.16	0.21	2.39	0.80

4.5. Correlation between average corrected velocity of Shear-wave (Vsl) and Ratio of Cyclic Resistance (CRR)

The correlation between Average corrected velocity of shear-wave, (Vsl), and Cyclic Resistance Ratio (CRR) (Table 2) can be seen in Fig. 13. This plot shows the dependence of CRR with Vsl as CRR = 0.0018Vsl - 0.1641. This is a linear relationship with strong coefficient of Regression, $R^2 = 0.9991$. This implies thatcyclic resistance ratio varies directly with shear-wave velocity.

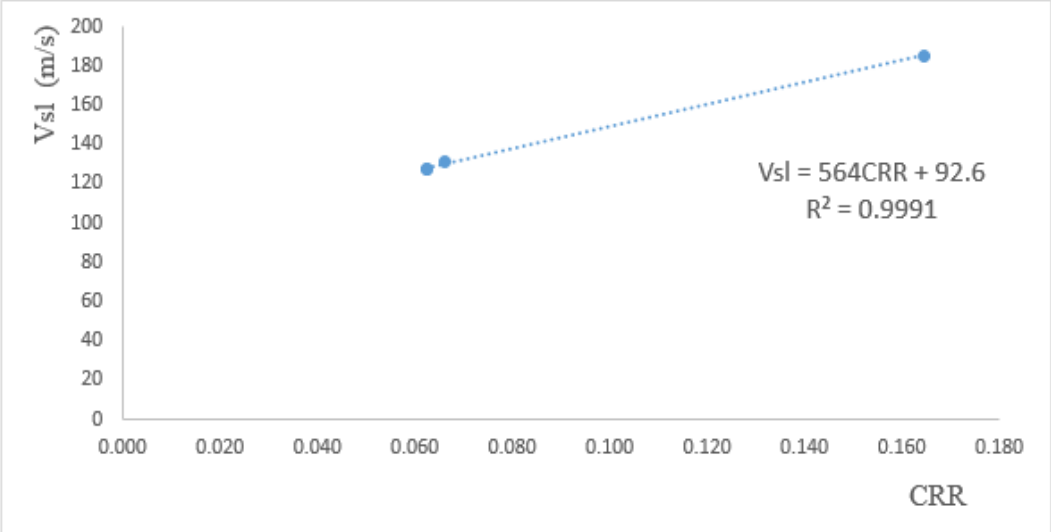

Fig 13: Relationship between average corrected velocity of shear-wave (Vsl) and ratio of cyclic resistance (CRR).

4.6. Relationship between average corrected shear-wave velocity (Vsl) and factor of safety (FS)

The graphical relationship between the average corrected shear-wave velocities (Vsl) and the safety factor (FS) (Table 2) is shown in Fig. 14. The relation is Vsl = 112.24FS + 94.889 with a coefficient of regression, $R^2 = 0.9908$. This is a linear relationship showing that increase in shear-wave velocity causes a rise in the factor of safety, thereby proving that as the depth from the surface increases downward, it is normal for shear-wave velocities to increase downward too. Nevertheless, this leads to the increasing capacity for soils to resist liquefaction.

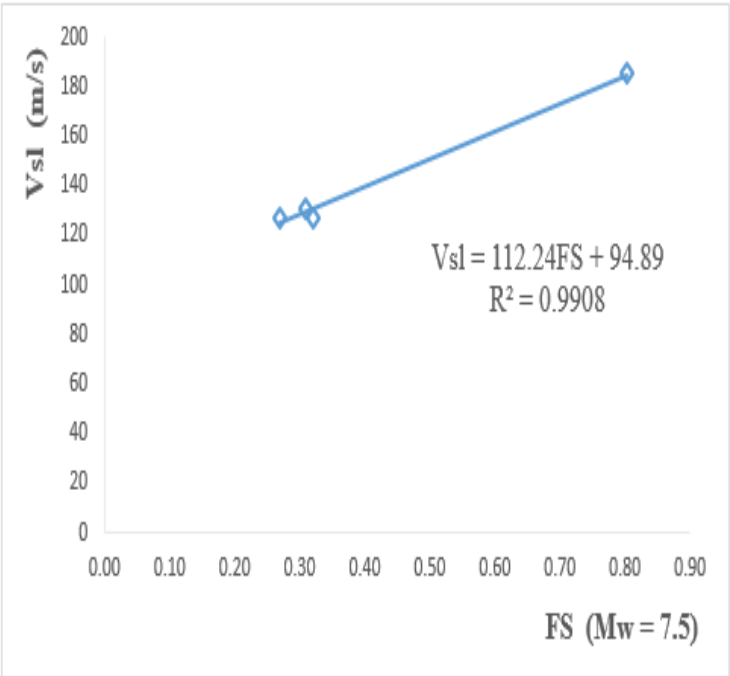

Fig 14: Relationship between average corrected shear-wave velocity (Vsl) and factor of safety (FS)

5.1. Conclusion

In this study, soil liquefaction susceptibility in Opoloarea of Bayelsa state was investigated.

The data from seismic refraction was interpreted using Time – intercept and general reciprocal methods. The result which also includes a 2D velocity model of the study area, validated the geological sequence.

The parameters for the Liquefaction were calculated within a depth interval of 8 m and 15 m, e.g., the cyclic stress ratio, the cyclic resistance ratio (sediment resistance) and the safety factor (cyclic resistance ratio/cyclic stress ratio).

Based on the Seismic refraction method, the cyclic stress ratio (CSR) is the same as that of electrical resistivity method. The ratio of cyclic resistance (CRR) was determined with the aid of Andrus and Stokoe, (1997) relation , The result show that the cyclic resistance ratio (CRR) in Opolo site are 0.063 and 0.164 for 8 m and 15 m respectively. The factor of safety at Mw = 5.5 in Opolo location is 0.804 (8 m) and 2.391 (15 m), while factor of safety at Mw = 7.5 is 0.270 and 0.802 for 8m and 15 m respectively.

Seismic refraction results show that in tremors or earthquakes with Magnitude of 5.5 (Mw = 5.5), soil at 8 m depth is susceptible to liquefaction due to its safety factor (0.804) been less than one while the soil at 15 m depth is not susceptible to liquefaction. Inearthquakes with Magnitude of 7.5 (Mw = 7.5), soils at both depth (8 m and 15 m) in the location are prone to liquefaction.

REFERENCE

[1]. Akinshipe R. B., Kenneth S. O. and Geoffrey C. S. O. (2021). Determination of elastic moduli and bearing capacity of sediments using geophysical and cone penetration test techniques in Yenagoa, Southern Nigeria, NRIAG Journal of Astronomy and Geophysics. 1 – 17.

[2]. Akpokodje, E. U. (1986). The engineering-geological characteristics and classification of the major superficial soils of the Niger Delta. Journal of Engineering Geology, 23,193 – 201.

[3]. Akpokodje, E. U. and Etu-Efeotor J. O. (1987), The occurrence and Economic potential of clean sand deposits of the Niger Delta, Journal of African Earth Science, 6, 61 – 65.

[4]. Amajor, L. C. (1991), Aquifers in the Benin Formation (Miocene-Recent), Eastern Niger Delta, Nigeria. Lithostratigraphy, Hydraulics and water quality. Journal of Environmental Geology and Water Science, 17, 85–101.

[5]. Anbazhagan, P. (2009). Liquefaction hazard mapping of Bangalore. Disaster Advances, 2(2), 26–35.

[6]. Andrus, R. D., Stokoe, K. H., Chung, R. M., and Juang, C. H. (2003). Guide for shear-wave-based liquefaction potential evaluation, Earthquake Spectra, 20 (2), 285.

[7]. Andrus, R. D., and Stokoe, K. H. (1997) Liquefaction resistance based on shear wave velocity, NCEER Workshop on Evaluation of Liquefaction Resistance of Soils, Salt Lake City, UT, Technical Report NCEER-97-0022, T. L. Youd and I. M. Idriss, eds., National Center for Earthquake Engineering Research, Buffalo, NY, 89–128.

[8]. Asokhia, M. B. (1984) Profile shooting and Data corrections in Dipping Beds at Akoka. Nigerian institute of Physics Bulletin, 6.

[9]. Beroya, M. A. A. and Aydin, A., (2007), First-level liquefaction hazard mapping of

[10]. Firat, S., Arman, H. and Kutanis, M. (2009). Assessment of liquefaction susceptibility of Adapazari City after 17th August, 1999 Marmara earthquake. Scientific Research and Essay. 4, 1012 - 1023.

[11]. Iwasaki, T., Tokida, K., Tatsuoka, F., Watanabe, S., Yasuda, S. and Sato, H. (1982) "Microzonation for soil liquefaction potential using simplified methods," in Proceedings of the 2nd International Conference on Microzonation, 1319–1330, Seattle, Wash, USA.

[12]. Liao, S. S. and Whitman, R., (1988), Regression Models For Evaluating Liquefaction Probability, Journal of Geotechnical Engineering, 114(4).

[13]. Mbonu P. D. C., Ebeniro, J. O., Ofoegbu, C. O. and Ekine, A. S. (1991), Geoelectric sounding for the determination of aquifer characteristics in parts of Umuahia area of Nigeria. Geophysics 56, 84–291.

[14]. Mollamahmutoglu, M., Kayabali, K., Beyaz, T. and Kolay, E. (2003). Liquefaction-related building damage in Adapazari during the Turkey earthquake of August 17, 1999. Journal of Engineering Geology. 67, 297 - 307.

[15]. Nwankwoala H. O.1 and Orji O. M. (2018). An Overview of Earthquakes and Tremors in Nigeria: Occurrences, Distributionsand Implications for Monitoring; International Journal of Geology & Earth Science, 4(4).

[16]. Okiongbo, K. S., Oboshenure, K. K., and Amakiri, A. R. C. (2019), Investigation of lithological control of iron enrichment in groundwater using geophysical techniques in Yenagoa, Southern Nigeria; SN Applied Sciences. 2, 107.

[17]. Ozcep, F., Karabulut, S., Özel, O., Ozcep, T., İmre, N., Zarif, H. (2014) Liquefaction-induced settlement, site effects and damage in the vicinity of Yalova City duringthe1999 Izmit earthquake, Turkey, Journal of Earth Syst. Sci. 123(1), 73 – 89.

[18]. Rami, K. A. R. I. (2014), Using Seismic Refraction Method to Investigate The Shallow Geologic Structures at Ayer Hangat Area, Langkawi, Malaysia. MSc. thesis, School of Physics, Universiti Sains Malaysia (USM).

[19]. Sahar, R. and Fereydoun, R. (2015), Evaluation of liquefaction potential of soil using the shear-wave velocity in Tehran, Iran, Springer Journal,

[20]. Shahri, A. A., Esfandiyari, B. & Rajablou, R. (2012), A proposed geotechnical-based method for evaluation of liquefaction potential analysis subjected to earthquake provocations (case study: Korzan earth dam, Hamedan province, Iran). Arab Journal of Geoscience, 5, 555 – 564.

[21]. Seed H. B. and Idriss, M. I. (1971), Simplified procedure for evaluating soil liquefaction potential, Journal of the Soil Mechanics and Foundations Division, 97(9), 1249–1273.

[22]. Short, K. C and Stauble, A. J. (1967), Outline of the geology of the Niger Delta. Bull AAPG 51,761–779

[23]. Song, C. R., and Mikell, N. (2013), Earthquake and Piping Hazard Assessment for Desoto, Tunica, and Tate County, Mississippi. Department of Civil Engineering, University of Mississippi.

[24]. Uko D. E., Ekine, A. S., Ebeniro, J. O., Charles O. Ofoegbu, C. O. (1992), Weathering structure of the east-central Niger Delta, Nigeria. Geophysics, 57(9), 1228–1233.

[25]. Yilmaz, I. and Yavuzer, D. (2005), Liquefaction potential and susceptibility mapping in the city of Yalova, Turkey. Journal of Enviromental Geology, 47, 175–184.